High efficiency domain wall gate in ferromagnetic nanowires

Dorothée Petit, Ana-Vanessa Jausovec, Huang T. Zeng, Emma Lewis, Liam O'Brien et al.

Citation: Appl. Phys. Lett. **93**, 163108 (2008); doi: 10.1063/1.3005586
View online: http://dx.doi.org/10.1063/1.3005586
View Table of Contents: http://apl.aip.org/resource/1/APPLAB/v93/i16
Published by the American Institute of Physics.

High efficiency domain wall gate in ferromagnetic nanowires

Dorothée Petit,[a)] Ana-Vanessa Jausovec, Huang T. Zeng, Emma Lewis, Liam O'Brien, Dan Read, and Russell P. Cowburn
Nanoscale Magnetics group, Department of Physics, Blackett Laboratory, Imperial College London, Prince Consort Road, London SW7 2BW, United Kingdom

(Received 16 August 2008; accepted 1 October 2008; published online 20 October 2008)

A transverse domain wall (DW) switchable gate with a very high efficiency is experimentally demonstrated in Permalloy nanowires using a transverse T-shaped structure. DWs are found to either travel undisturbed through the open gate or to be strongly trapped in front of the closed gate only able to travel backwards. The opening and closing of the gate depends on the magnetic configuration of the gate and is controlled using externally applied magnetic fields. Micromagnetic simulations confirm the experimental results. © *2008 American Institute of Physics*. [DOI: 10.1063/1.3005586]

Domain walls (DWs) are known to be pinned by topographical changes in an otherwise straight magnetic nanowire. Whether the topographical change takes the form of a (symmetrical or asymmetrical) protrusion,[1–3] a (symmetrical or asymmetrical) constriction,[1,4,5] or a pair of wires,[6] a DW will experience a modification of the potential lanscape in its vicinity and will therefore see its propagation field change. Understanding and controlling DW propagation in nanowires is at the core of DW based logic and memory devices.[7,8] A switchable DW gate has been demonstrated[6] for vortex DWs, which, under the same applied field condition and under user control, can either be open and let DWs through or be closed and block the passage of DWs. The efficiency of such a gate depends on the discrimination between the transmission fields of a DW in the open and the closed states of the gate, but also on how low the transmission field in the open state is, so that the presence of an open gate would be as little disruptive as possible if placed in a complex magnetic circuit. In this paper, we experimentally and numerically demonstrate that a transverse arm (TA) placed on one side of a DW conduit acts like a very high efficiency gate. We find that a DW either travels almost unperturbed through the open gate or is so strongly trapped in front of the closed gate that it transmits through the gate at a field only slightly below the field required to switch the other side of the gate via nucleation of a new domain. The opening and closing of the gate depends on the micromagnetic configuration in the gate and is controlled by external magnetic fields.

200 nm wide nanowires were milled using focused 30 keV Ga^+ ions from a 7 nm thick, thermally evaporated $Ni_{80}Fe_{20}$ film on Silicon substrate. 200 nm wide, 2 μm long perpendicular arms were patterned in the same milling process. One end of each structure was shaped into a C for DW creation (see the top of Fig. 1). High sensitivity, spatially resolved magneto-optical Kerr effect (MOKE) measurements were used to study experimentally the switching properties of the structures. Global 45° reset field pulses were used to control the magnetization in the TA and create DWs in the C part of the structure. The bold arrows in Fig. 1 show the directions of the applied field. H^{P}_{reset} [Fig. 1(a)] creates a DW in the bottom corner of the C and resets the magnetization in the TA downwards. In this case, the magnetization in the core of the DW and in the magnetization in the TA are parallel (P). The field is then reduced at 45° to a 10 Oe y offset of the same sign as the reset field pulse (to ensure that the DW remains in the bottom of the structure). The x component of the field is subsequently reversed in order to push the DW toward the trap [Fig. 1(b)]. H^{AP}_{reset} (Fig. 1(c)) creates a DW in the top corner of the C and resets the magnetization in the TA upwards. The field is then reduced at 45° to a 10 Oe y offset of the opposite sign to the reset field pulse (to push the DW to the bottom of the structure). The x component of the field is subsequently reversed in order to push the DW toward the trap [Fig. 1(d)]. In this case, the magnetization in the core of the DW and the magnetization in the TA are antiparallel (AP). Figure 2 shows the time evolution of the x component of the applied magnetic field (a), together with the corresponding MOKE traces measured before [(b) and (d)] and after [(c) and (e)] the TA. The orientation of the TA and the part of the structure where the loop was measured are indicated in the insets. The DW is created during the negative part of H_x and pushed during the positive part. When the MOKE laser spot is placed before the gate, sharp transitions are observed in both the P and AP cases when H_x reaches the

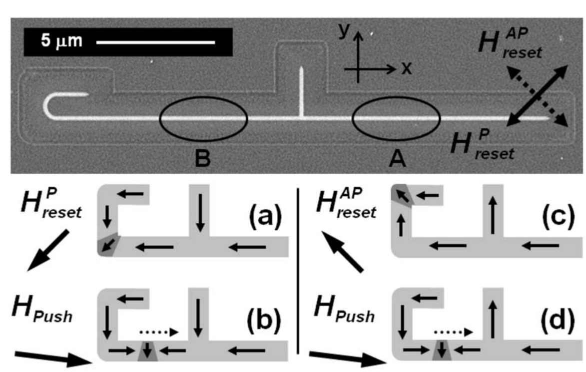

FIG. 1. Top: secondary electron image by FIB irradiation of a 200 nm wide Permalloy structure with a DW gate at its middle. Ellipses A and B show the two positions of the laser beam during MOKE measurements. The double arrows show the directions H^{P}_{reset} and H^{AP}_{reset}. Bottom: schematics illustrating the field sequences used to measure the switching properties of the structures. (a) and (b) illustrate the creation and displacement of a head to head DW in the P configuration. (c) and (d) show the AP configuration. The large arrows indicate the direction of the external magnetic field, the narrow arrows show the direction of the magnetization in the nanostructure, and the dotted arrows show the direction of displacement of DWs.

[a)]Electronic mail: d.petit@imperial.ac.uk.

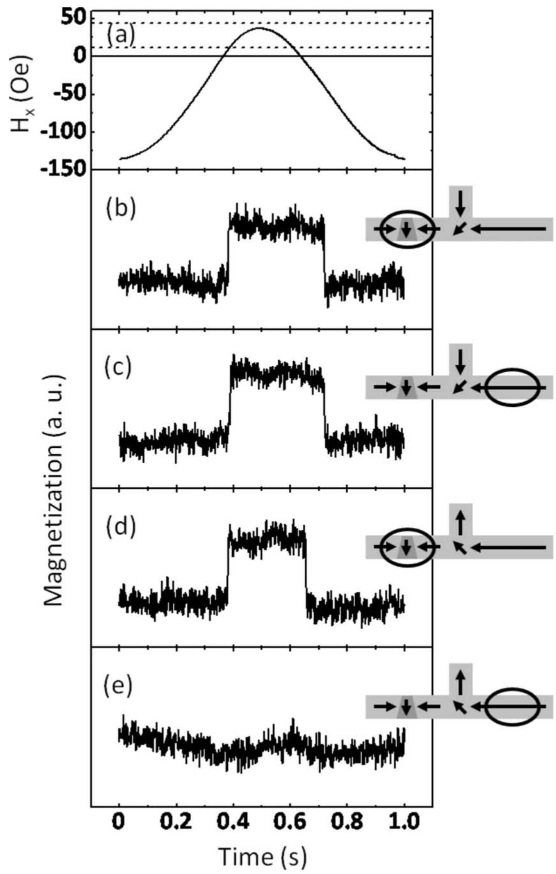

FIG. 2. Horizontal field H_x (a) and MOKE traces [(b)–(e)] measured before the gate [(b) and (d)] and after the gate [(c) and (e)] when the magnetization in the core of the incoming DW is P to the magnetization in the gate [(b) and (c)]; and AP [(d) and (e)]. The DW is created during the negative part of H_x and pushed toward the trap during the positive part. The upper dotted line in (a) indicates H_T^{P}, the lower one H_T^{AP}.

propagation field H_{P}=7 Oe [left transitions in Figs. 2(b) and 2(d)], showing that a DW has been created which succesfully propagates toward the gate. When the laser spot is placed on the other side of the gate [Fig. 2(c) and 2(e)], different behaviors are observed, depending on the orientation of the magnetization in the TA. In the P case (c), a sharp transition is observed when H_x reaches H_T^{P}=10 Oe [lower dotted line in Fig. 2(a)], whereas no switching is seen in the AP case (e) as long as the maximum field used to push the DW does not exceed 43 Oe [upper dotted line in Fig. 2(a)]. The TA does indeed act as a gate. For the same value of the external field in the range 10–43 Oe, it is closed when its magnetization is AP to the magnetization inside the core of the DW, and open when P. Furthermore, the DW travels through the open gate at an applied field only 3 Oe higher than H_{P}: the presence of an open gate causes very little disruption. As H_x is reversed in the open (P) configuration, a sharp transition is observed at −43 Oe on both sides of the gate [right transitions in Figs. 2(b) and 2(c)]. Sharp transitions at $H_N = \pm 43$ Oe are also observed when no DW is initially present in the horizontal arm of the structure, showing that the DW in the P case has indeed transmitted through the gate and anihilated at the end of the wire, so that a new domain has to nucleate in order to switch the structure. In the closed (AP) case, switching of the left hand side of the nanowire [before the gate - right transition in Fig. 2(b)] is measured at −9 Oe when H_x is reversed. This low $\sim H_{\mathrm{P}}$ switching value shows that the original DW is

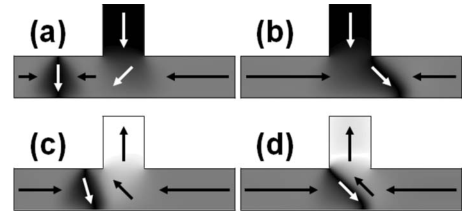

FIG. 3. OOMMF calculated micromagnetic configurations when a head to head DW approaches the gate in the open P configuration [(a) and (b)] and in the closed AP configuration [(c) and (d)]. (a): H_x=15 Oe, this in not an equilibrium configuration and the DW was slowly moving away from the gate despite the applied field; (b): H_x=20 Oe; (c): H_x=0; (d): H_x=110 Oe. H_y=20 Oe in all cases. (b) and (d) show the last equilibrium configuration before the right hand side of the structure switches for a 5 Oe higher applied field.

indeed still present in front of the closed gate, able to back propagate as soon as a negative field of the order of the propagation field is applied.

Micromagnetic simulations were performed using the OOMMF package[9] ($M_S = 800 \times 10^3$ A/m, $A = 13 \times 10^{-12}$ J/m, $3.5 \times 3.5 \times 7$ nm^3 cell size). The simulated area extended 1 μm away from the gate in all directions. The simulations were performed quasistatically, with α set to 0.5 to speed up the calculations. Transverse DWs are stable for our geometry and DW creation method.[1,10–12] A downward head to head DW was artificially placed next to the gate, and left to relax under the smallest horizontal field required so that the long range magnetostatic interaction between the gate and the DW does not cause the DW to move away from the gate [an applied field of 17.5 ± 2.5 Oe was necessary to overcome the repulsion between the positively charged DW and the positively charged junction in the P case, see Fig 3(a)]. The horizontal field was then increased in 5 Oe steps, until the right hand side of the nanowire switched. Figure 3 shows the micromagnetic configurations calculated as the same downward DW is approaching a gate in the open (P) state (a), and in the closed (AP) state (c), and just before the right hand side of the structure switches [(b) and (d)]. The simulations show that when the gate is in the open state, the DW simply enters the gate at $H_x = 17.5 \pm 2.5$ Oe, where it remains trapped until H_x reaches the transmission field $H_T^{\mathrm{P}} = 22.5 \pm 2.5$ Oe, at which point the DW travels past the gate and switches the right hand side of the structure. Figure 3(b) shows the micromagnetic configuration under 20 Oe applied field. In the closed state, the DW is strongly pinned in front of the AP gate. In order to propagate past the gate, the DW has to reverse the TA, which happens at $H = 112.5 \pm 2.5$ Oe, when the original DW splits into two DWs, one which travels up and reverses the TA, and one which travels through the gate and reverses the other side of the structure. Figure 3(d) shows the micromagnetic configuration under 110 Oe applied field. A transverse H_y field of 20 Oe was applied in both the P and AP cases to mimic the experimental ±10 Oe transverse field required in the experiment to move the DW in the bottom arm — the vertical field has been multiplied by two in the simulations to scale with the doubling of H_T^{P} field in the P case between experiments and simulations. The qualitative agreement between experiments and simulations is excellent, and confirm the findings of Ref. 1, namely that the relative orientation between the magnetization in the core of the transverse DW and the micromagnetic configuration at the trap is a fundamental parameter to describe the pinning properties of a given trap. The gate property is seen in the simulations, where a DW with core magnetization P to the magnetizationin the gate travels through at a much lower field (22.5 ± 2.5 Oe) than a DW with core magnetization AP to the magnetization in the gate. The simulations also confirm that a DW in the AP case remains trapped in front of the closed gate. If the horizontal component of the field is reversed before the right hand side of the structure has switched, then the DW can be pulled back from the front of the gate with a reverse field of 7.5 ± 2.5 Oe. This nonzero value is not due to a nonzero propagation field in the simulated wire, as no edge roughness has been included in the calculation. It is rather due to the attractive magnetostatic interaction between the positively charged DW and the negatively charged junction. This interaction was also seen experimentally where a reverse field 2 Oe higher than H_P was needed to pull the DW back from the closed gate. Direct quantitative agreement between experiments performed at room temperature and simulations performed at zero temperature is not expected,[13] and the simulated switching fields are on average 50% higher than the experimental ones.

As a summary, we have demonstrated experimentally and numerically that a perpendicular arm placed on one side of a DW conduit acts as a DW gate, either letting DWs travel through with very little perturbation or completely blocking DWs in front of it. The gate is controlled by external applied fields via its magnetic configuration. It is open when its magnetization is P to the magnetization in the core of the incoming DW and closed when AP. In the closed state, we have shown that the DW is blocked in front of the gate from where it can be pulled back using a low horizontal field.

This work was supported by the European Community under the Sixth Framework Programme SPINSWITCH (MRTN-CT–2006–035327).

[1]D. Petit, A.-V. Jausovec, D. Read, and R. P. Cowburn, J. Appl. Phys. **103**, 114307 (2008).
[2]M. T. Bryan, T. Schrefl, and D. A. Allwood, Appl. Phys. Lett. **91**, 142502 (2007).
[3]D. A. Allwood, G. Xiong, and R. P. Cowburn, Appl. Phys. Lett. **85**, 2848 (2004).
[4]C. C. Faulkner, M. D. Cooke, D. A. Allwood, D. Petit, D. Atkinson, and R. P. Cowburn, J. Appl. Phys. **95**, 6717 (2004).
[5]J. Grollier, D. Lacour, V. Cros, A. Hamzic, A. Vaurès, A. Fert, D. Adam, and G. Faini, J. Appl. Phys. **92**, 4825 (2002).
[6]M. Hara, J. Shibata, T. Kimura, and Y. Otani, Appl. Phys. Lett. **89**, 192504 (2006).
[7]D. A. Allwood, G. Xiong, M. D. Cooke, C. C. Faulkner, D. Atkinson, N. Vernier, and R. P. Cowburn, Science **296**, 2003 (2002).
[8]D. A. Allwood, G. Xiong, C. C. Faulkner, D. Atkinson, D. Petit, and R. P. Cowburn, Science **309**, 1688 (2005).
[9]The OOMMF code is available at http://math.nist.gov/oommf.
[10]R. D. McMichael and M. J. Donahue, IEEE Trans. Magn. **33**, 4167 (1997).
[11]Y. Nakatani, A. Thiaville, and J. Miltat, J. Magn. Magn. Mater. **290**, 750 (2005).
[12]M. Laufenberg, D. Backes, W. Bührer, D. Bedau, M. Kläui, U. Rüdiger, C. A. F. Vaz, J. A. C. Bland, L. J. Heyderman, F. Nolting, S. Cherifi, A. Locatelli, R. Belkhou, S. Heun, and E. Bauer, Appl. Phys. Lett. **88**, 052507 (2006).
[13]A. Himeno, T. Okuno, T. Ono, K. Mibu, S. Nasu, and T. Shinjo, J. Magn. Magn. Mater. **286**, 167 (2005).